

**EFFECTS OF END PLATES ON RESOLUTION  
OF WIRE CHAMBERS\***

**BILL R. BAKER**

*Stanford Linear Accelerator Center*

*Stanford University, Stanford, California 94305*

**Abstract**

Resolution may be significantly degraded near conducting end plates of wire chambers. Simple analytic methods are used to estimate the field distortion and consequent changes in drift time.

Submitted to Nuclear Instruments and Methods

---

\* Work supported by the US Department of Energy under DE-AC03-76SF00515

## 1. Introduction

Conducting end plates affect the field near the ends of wire chambers and generally degrade the resolution. For a case such as the SLD central drift chamber, which is to be operated with all field shaping wires at potentials below that of the end plates, the nominal resolution may be lost for several per cent of the chamber length. Presence of the grounded plate distorts the field causing local variations in the drift speed in an unsaturated gas. Electrons freed near the end plate drift to it and never reach the sense region back of the guard wires. Methods for estimating the distortion are given here, and some proposals to reduce the effects are studied.

## 2. Model

The region near the junction of a cell with the end plate is sketched in fig. 1a. Boundaries of the cells fall along radial or circumferential arcs of the circular end plate. The so-called guard wires are operated at  $-3.4$  kV while the radial line of field wires are at an average potential of about  $-6.8$  kV. Since the radial edges of the cell are slightly inclined the voltages of the individual field wires are also graded to provide a more uniform drift field for any electrons released in either side of the cell. Additional field shaping wires, lying along arcs at constant radius and shown as light lines in fig. 1a, are also supplied with voltages chosen to improve the uniformity of the drift field. Because of the essentially two dimensional character of the field a good representation of the effects of the end plate can be derived from a simple problem in the  $x, y$ -plane sketched in fig. 1a.

Nominal potentials are  $-6.8$  kV and  $-3.4$  kV, but it is shown in the Appendix that parallel sets of wires at those potentials result in a central field far from the end plate corresponding to solid planes at  $-5100 \pm 1509$  V. Then the fields near the plate can be discussed in terms of the problem of fig. 1b where the field wires are represented by a constant potential plane on the left, the guard wires by a constant potential on the right and where zero potential on the bottom end represents the plate. The spacing between field and guard wires is about 26 mm giving a nominal field,  $E_0 \approx 1161$  V/cm, far from the end disturbances.

A normalized form of the problem is sketched in fig. 1b where the semi infinite strip  $-1 \leq x \leq 1$ ,  $0 \leq y \leq \infty$  in the  $z$ -plane has boundary potential  $V = -1, A$ , and  $+1$  respectively on the left, bottom, and right hand sides. For the voltages of the SLD CDC the normalized end value would be  $A \approx 3.379$ . The normalized coordinates and boundary values are enclosed in parentheses in fig. 1b.

The normalized voltage,  $V$ , can be taken as the real part of a complex potential

$$F(z) = V(x, y) + iC(x, y) \quad , \quad (1)$$

and  $C$  is the complementary function whose level curves are the field lines. Conformal transformation by the function

$$\zeta = \sin\left(\frac{z\pi}{2}\right) \quad (2)$$

maps the semi-infinite strip of the  $z$ -plane onto the upper half of the  $\zeta$ -plane of fig. 1 d. The potential  $V$  is piecewise constant along the edge of that half plane with discontinuities at points  $\xi_k$ ,  $k = 1, 2, \dots, M$  obtained from eqn. 2. By inspection the solution in the transform plane is

$$F(\zeta) = V_M - \frac{i}{\pi} \sum_{k=1}^M (V_{k-1} - V_k) \ln(\zeta - \xi_k) \quad (3)$$

where  $V_k$  is the boundary value on  $\xi_k < \xi < \xi_{k+1}$  and  $V_0$  is the value on  $\xi < \xi_1$ . The branch cuts are in the lower half plane, and the logarithm is real for real arguments.

The last two equations give a parametric solution in terms of the physical coordinate  $z$ . Equipotentials and field lines are shown in the examples of fig. 2 for two values of the end plate potential.

An interesting feature of fig. 1b and fig. 2a is the bifurcation point  $b$  where the equipotential from the lower left corner splits to form the right hand boundary at potential  $V(1, y) = +1$ . From eqn. 3 the height of point  $b$  is

$$y_b = \frac{2}{\pi} \cosh^{-1} A \approx 1.202 \quad (4)$$

There is also a significant limiting fieldline from the point  $c$  on the left wall to the bifurcation point  $b$ . All electrons released below that curve will drift to the end plate and not to the guard wires. In addition to that loss the field just above the dead zone is greatly distorted.

It would be desirable to have a uniform field in the strip so the potential on the end should also vary linearly with  $x$ . Such a smooth function is difficult to implement, but  $N = M - 1$  discrete conducting pads might be placed inside the end to approximate the uniform gradient. An example is shown in fig. 1c where three equal steps with two break points

$$x_{k+1} = -1 + 2k/N, \quad k = 1, \dots, N-1 \quad (5)$$

and potentials

$$V_k = -1 + (2k-1)/N, \quad k = 1, \dots, N \quad (6)$$

are used.

Equipotentials and field lines are plotted in fig. 3 for  $N = 1$  and 3. The case  $N = 1$ , fig. 3a, gives the mean potential,  $V = 0$ , on  $y = 0$ . For large  $y$  the field lines between the left and right sides are nearly parallel to the  $x$ -axis. However, near the corners of the strip, field lines connect the halves of the end to the nearest wall. Therefore electrons released in the dead zone in the lower left corner would be swept to the end while those freed in the lower right corner drift to the right wall with appreciable motion away from the end. From eqn. 3 it can be shown that the dead zone extends along the left wall to height

$$y_c = \frac{2}{\pi} \cosh^{-1} \sqrt{2} \approx .5611 \quad (7)$$

Examination of fig. 3 reveals the fundamental scaling law for this problem: placing  $N$  pads on the end in the given manner just divides the original strip into

$N$  similar smaller ones. In this case similar means that linear dimensions scale as  $1/N$  and that potential differences between corresponding points also vary as  $1/N$ . It is easier to recognize that fact for  $N = 2$  where symmetry about the  $y$ -axis is obvious. Next it can be extended to cases where  $N = 2^p$ , a simple binary number. For the general case it is convenient to think of  $N$  disjoint strips with potential differences of  $2/N$  between the two walls and  $\pm 1/N$  between the end and the sides. The fluxes or fields at a given height  $y$  on the two sides are equal in magnitude but of opposite sign so the  $N$  strips can be compatibly joined as in the original problem.

The scaling law also means that the fields are the *same* at corresponding points, so the fields for any number  $N$  of pads can be found at the corresponding point of the case with  $N = 1$ . Curves of fig. 4 show the variation of the horizontal field component along lines at fixed values of  $y$  for the case  $N = 1$ . Those curves give an impression of the variation of the field. Details of the electron paths, or field lines, are considered in the next section.

### 3. Resolution

If the relatively small effect of the magnetic field is neglected then free electrons drift along electric field lines toward higher potential with velocity proportional to the ratio of field to gas density,

$$\frac{d\vec{s}}{dt} = \vec{v} = -\frac{k}{\rho} \vec{E} \quad . \quad (8)$$

Infinitely far from the end the field approaches a uniform state with amplitude  $E_\infty$ , and speed

$$v_\infty = -\frac{k}{\rho} E_\infty \quad . \quad (9)$$

The transit time from a source point along its field line to an exit at the sense region past the right hand wall of the strip is,

$$t_{exit} - t_{source} = -\frac{\rho}{k} \frac{h}{E_\infty} \int_{source}^{exit} \frac{d\vec{s}/h}{\vec{E}/E_\infty} = \frac{h}{v_\infty} \int_{source}^{exit} \frac{dz}{F'(z)} \quad (10)$$

where the integral is taken along the field line from source to exit, and, as before,  $x$ ,  $y$ , and  $z = x + iy$  are all normalized with respect to  $h$ , the half width of the strip. The apparent distance is the product of  $v_\infty$  with the transit time of eqn. 10, and the error relative to the half width is

$$\delta = [h - hx_s - v_\infty(t_{exit} - t_{source})]/h = 1 - x_s + \int_{exit}^{source} \frac{dz}{F'(z)} \quad (11)$$

The field line can be traced by integrating from the exit point on the right edge back along the curve  $dC = 0$  obtained from

$$dF = dV + idC = \frac{dF}{dz} dz = (C_{,y} + iC_{,x})(dx + idy) \quad (12)$$

At each point of the curve the values of  $F'(z)$  and  $x$  are saved. Then numerical integration is used to evaluate eqn. 11. Results are shown in fig. 5 for three cases of constant potential on the end.

An important measure of the extent of the disturbance near the end is the value of  $y_{exit}$  which gives a maximum error of  $100 \mu\text{m}$  in the apparent distance of the source. The dimensionless  $\delta$  would be  $100 \mu\text{m} / 13 \text{ mm} = 0.0077$ . From the summary curves of fig. 5 the corresponding values of the dimensionless exit distance are about 1.44, 3.23, and 4.02 corresponding to physical distances of 18.7, 42.0, and 52.3 mm for constant dimensionless end potentials of  $A = 0, 1.0, \text{ and } 3.379$  respectively. The scaling law described previously shows that the size of the disturbed region could be decreased by a factor  $1/N$  from the case  $A = 0$  if  $N$  pads were used to approximate a linear variation of the end potential. Details are not pursued here because of the difficulties of fabricating such a system.

In regions far from the end the field lines are nearly parallel to the  $x$ -axis, so  $F'(z) = V_{,x} - iV_{,y}$  is nearly 1, and a good approximation to eqn. 11 is

$$\begin{aligned} \delta &\approx 1 - x_s + \int_e^s \frac{dz}{1 + (F' - 1)} \approx 1 - x_s + \int_e^s [1 - (F' - 1)] dx \\ &\approx 1 - x_s + 2(x_s - 1) - V_s + V_e = x_s - V_s \end{aligned} \quad (13)$$

For the case of the end at the average of field and guard wire potentials, see fig. 3a,  $N = 1$ , the voltage decreases more rapidly than  $x$  near the right wall. Therefore the error  $\delta$  in the apparent distance is positive. However, for  $x_s \approx 0$  the approximation, eqn. 13, vanishes, and it changes sign for negative  $x_s$ . On field lines far enough from the end so that maximum  $\delta \leq .01$ , the approximation, eqn. 13, is accurate within about 5 per cent of the maximum value of  $\delta$  on the line.

#### 4. A single, smaller pad

The previous discussions concerned piecewise constant potential distributions on the end with break points at equally spaced intervals. Providing those distributions with discrete electrodes would be difficult, so it is interesting to estimate the effects of more easily constructed pads. The simplest case to build would be a single pad which does not quite fill the end. Questions of corona near the edges of such an insulated pad will be ignored, and the effect of the width will be studied.

The potential can still be found from eqn. 3 if a centered pad of half width  $p$  is held at potential  $B$ . An example is plotted in fig. 6a where a pad at potential  $B = 0$  occupies the central three quarters of the end. Outside the pad the end potential is again  $A = 3.379$  corresponding to the conditions of the SLD chamber.

The summary curves of fig. 7a show the resolution  $\delta$  on paths leaving the drift region at height  $y_{exit}$  for pads at zero potential and for the labeled half widths. Of course results shown for  $p = 0$  or  $p = 1.0$  agree with the limiting curves of fig. 5d. The value of  $y_{exit}$  at the limit of  $100 \mu\text{m}$  resolution is rather sensitive; increasing from 1.44 for  $p = 1.0$  to 2.39 for  $p = 0.75$ .

If the pad were the full width of the drift region,  $p = 1.0$ , then its optimum voltage is  $B = 0$ . However, for  $p < 1$  the portions of the end at  $A = 3.379$  can be more effectively balanced by using a negative value for  $B$ . Field and potential lines with  $B = -.28$  and  $p = .75$  are shown in fig. 6b. Plots of the resolution for more examples with the same half width  $p$  but various values of  $B$  are shown in fig. 7b. The resolution improves as  $B$  is decreased from 3.379, the potential of the end plate, until the value  $B = -.28$ . Then the resolution begins to worsen for more

negative  $B$  as shown by the curve for  $B = -0.5$ . The best resolution was computed for  $B \approx -.28$ , and the value of  $y_{exit}$  at the  $100 \mu\text{m}$  limit was 1.46, a very slight increase over the limit of 1.44 found for a complete end at  $A = 0$  as in fig. 3a.

## 5. Conclusions

Simple analytic methods can be used to study the disturbances due to various potential distributions on the end shell. For the voltages of the SLD Design Report a dead zone extends about 20 to 30 mm from the end, and position errors of  $100 \mu\text{m}$  would occur as far as 52 mm from the end. By adjusting voltages so that the end shell is at the mean of the field and guard wire potentials, the  $100 \mu\text{m}$  perturbations extend only about 19 mm into the cell. Adding pads to the end shell to approximate the ideal linear voltage variation with discrete steps could further reduce the distortion. However, simple, reliable methods for attaching and driving such electrodes have not yet been developed. Results such as those of fig. 5 might form the basis for software corrections to improve the resolution in the end regions.

## 6. Acknowledgment

The problem was posed by C. Prescott, and his suggestions and questions as well as those of H. Yamamoto and C. Young are greatly appreciated.

## Appendix A. Parallel Wires

Far from the end of the cell the drift region resembles the idealized geometry of fig. 8 imbedded in a complex  $w$ -plane. Guard wires are spaced at regular intervals  $a$  along the real axis, and field wires, at the same pitch, are at height  $2h$ . Each wire can be represented by an ideal line charge, and the complex potential is

$$F_p(w) = Q \left\{ \ln(w) - \ln(w - i2h) + \sum_1^{\infty} [\ln(w - na) + \ln(w + na) - \ln(w - na - i2h) - \ln(w + na - i2h)] \right\} . \quad (14)$$

By using the infinite product and partial fraction representations[1] of trigonometric functions it can be shown that the voltage at radius  $R$  on the surface of the wire centered at the origin is

$$\frac{V_{wire}}{Q} = -\ln \frac{\sinh \frac{2\pi h}{a}}{\frac{2\pi h}{a}} + \ln \frac{R}{2h} \quad , \quad (15)$$

and the vertical field component at  $(0, h)$  is

$$\frac{E_{ym}}{Q} = -\frac{2\pi}{a} \coth \frac{\pi h}{a} \quad . \quad (16)$$

Dimensions of the CDC are  $a = 5$  mm,  $h \approx 13$  mm,  $R = 0.1$  mm so eliminating  $Q$  between the two previous equations gives

$$\frac{E_{ym}}{V_{wire}} = \frac{.6830}{\text{cm}} \quad . \quad (17)$$

The corresponding field at the midpoint would be

$$E_{ym} = 1700 \times .6830 \text{ Volts/cm} = 1161 \text{ V/cm} \quad . \quad (18)$$

Replacing the wires of fig. 8 by planes at  $-5100 \pm 1509$  V would give the same gradient. If the voltages on those planes were normalized to  $\pm 1$  then the grounded end plate would be at a normalized potential of  $A = 5100/1509 = 3.379$ .

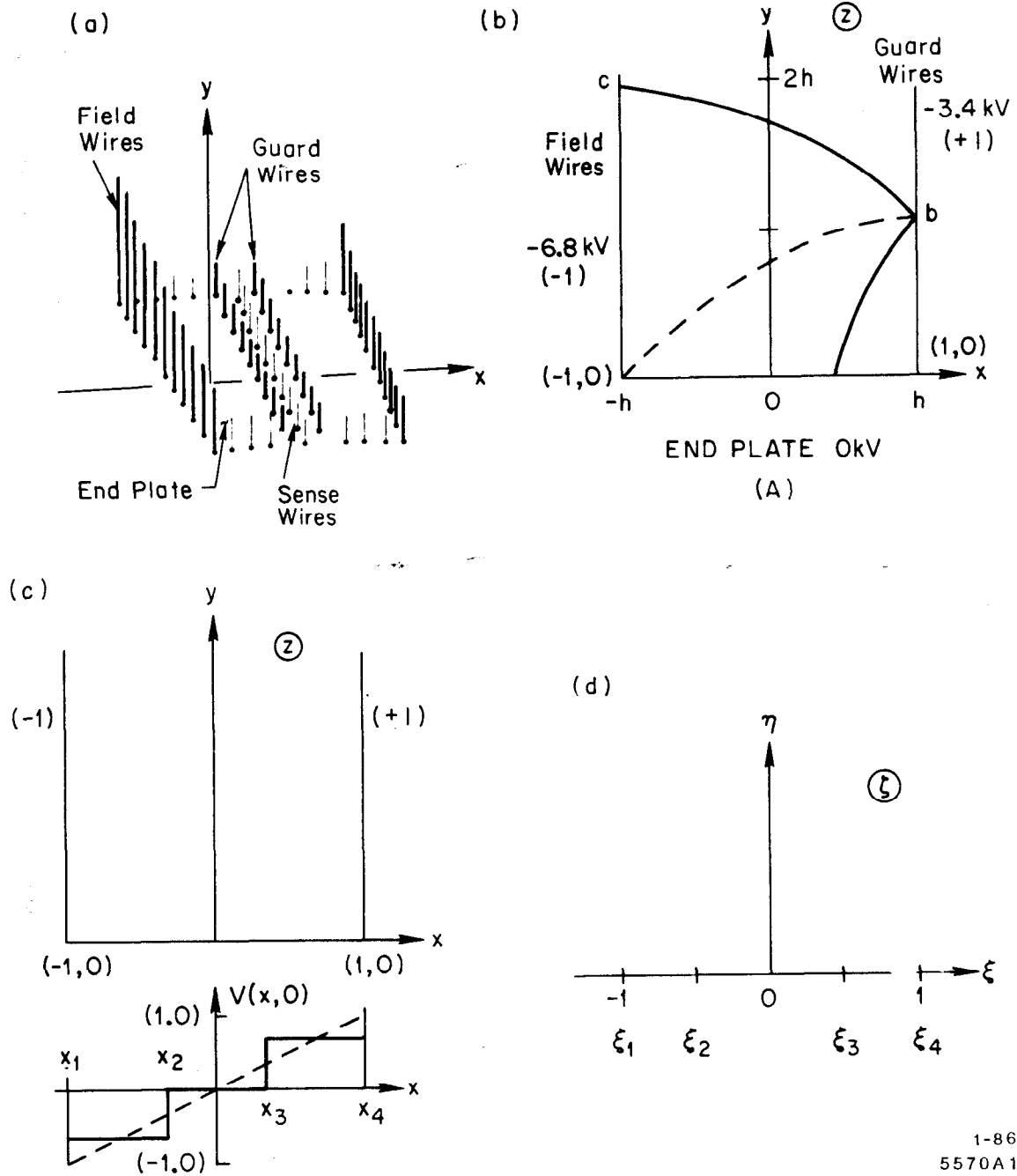
## REFERENCES

1. Abromowitz, M. and Stegun, I. A., editors, Handbook of Mathematical Functions, NBS Applied Mathematics Series 55, 1964.

## FIGURE CAPTIONS

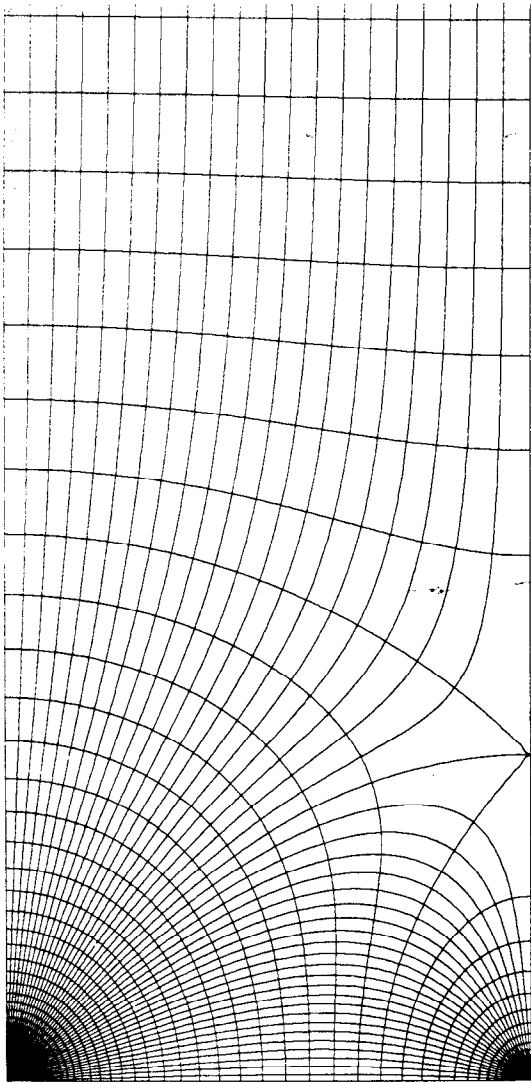
1. a. The end region at junction of a cell and the end plate. b. An approximate two dimensional representation of the drift zone near the grounded plate. c. A more favorable piecewise constant potential on the end. d. The transform plane.

2. a. Field and potential lines on the left are for the original SLD CDC configuration over the region  $-1 \leq x \leq 1$ ,  $0 \leq y \leq 4$ . b. The right side shows the end at the potential of the guard wires.
3. a. Field and potential lines on the left are for the end at the mean of the field and guard wire potentials. b. The right side shows the end with three equal steps in potential.
4. Transverse field component  $E_x$  at various heights,  $y = 0.1, 0.2, \dots, 1.0$  for the end at zero potential as in fig. 3a.
5. Resolution  $\delta$  is shown across the strip for field lines that exit at the given  $y$ -values. End potential  $A = 3.379$  corresponds to the original configuration of the SLD design Report,  $A = 1$  means the end is at the potential of the guard wires, and  $A = 0$  places the end at the mean of guard and field wire potentials. The last graph summarizes the maximum values of  $\delta$  occurring on field lines with given exit values.
6. a. Field and potential lines on the left are for a pad of width  $p = .75$  at potential  $B = 0$ . b. The right side shows the pad at potential  $B = -.28$ .
7. a. Resolution  $\delta$  for central pad at zero potential, half width  $p$  increasing from zero to fill the end. b. Central pad  $3/4$  of total width. Pad potential  $B$  ranges from that of remainder of end plate down to  $-0.5$ .
8. Infinite rows of guard wires at  $Im w = 0$  and field wires at  $Im w = 2h$ .



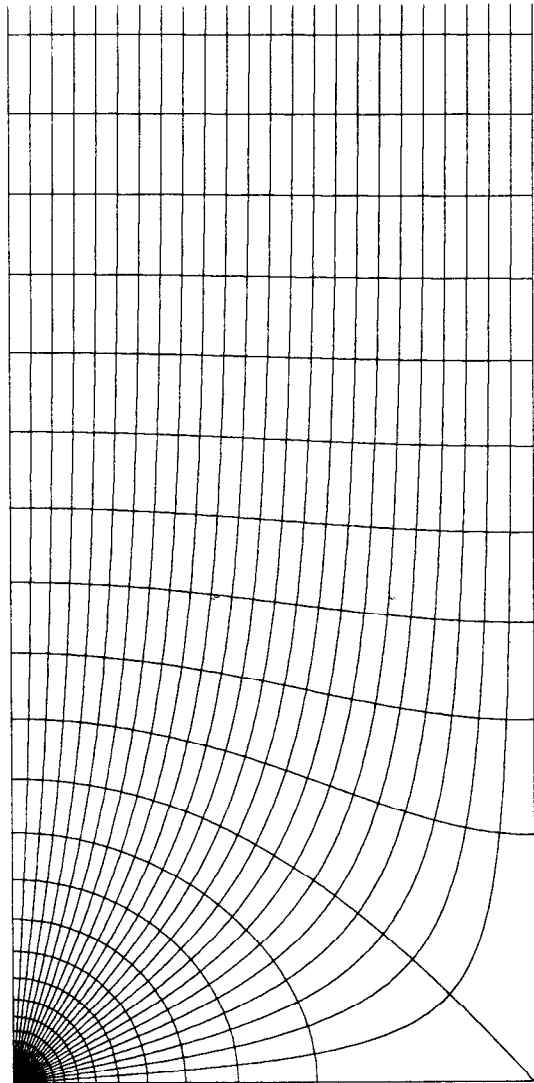
1-86  
5570A1

Fig. 1



$A = 3.379$

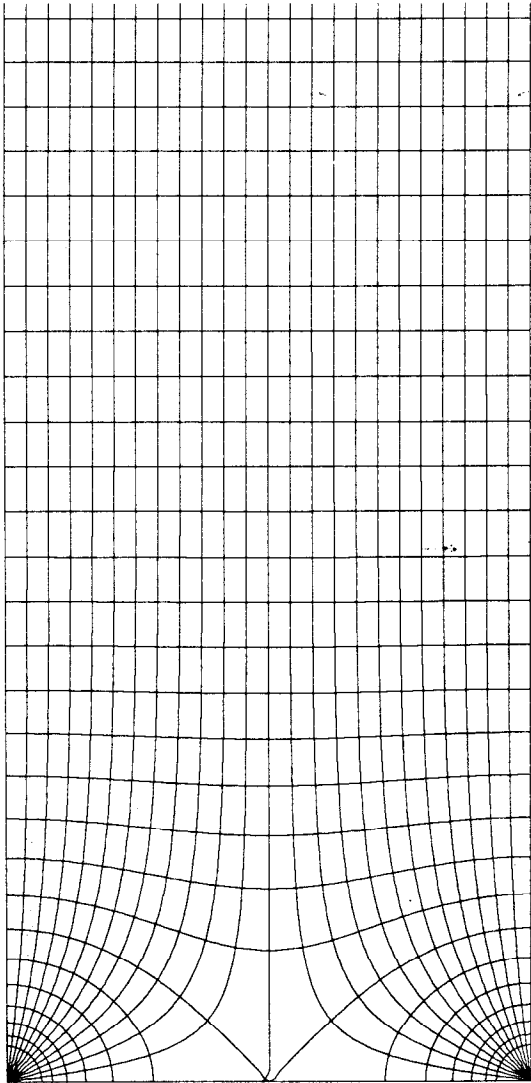
1-87



$A = 1.000$

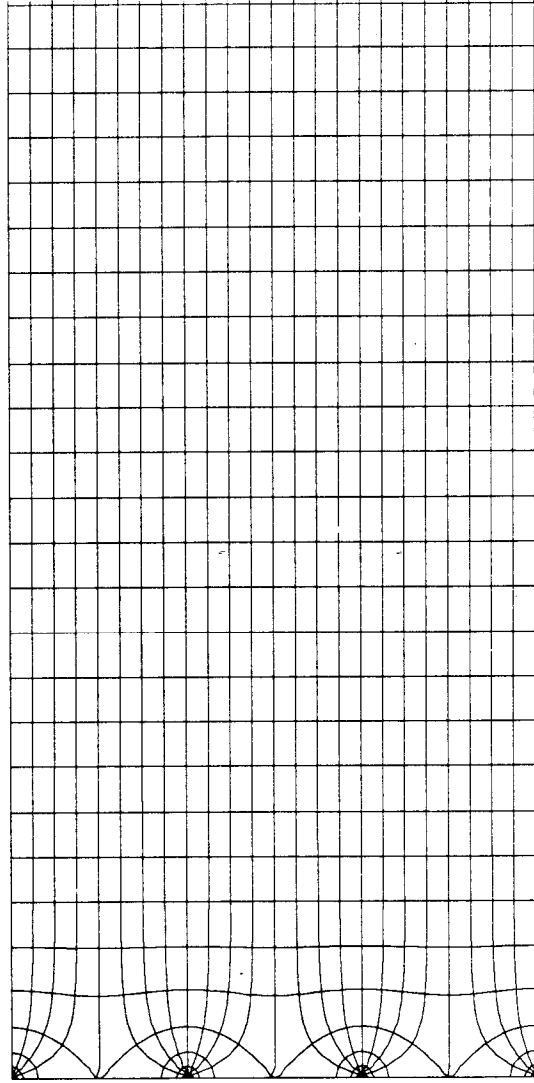
5570A2

Fig. 2



1-87

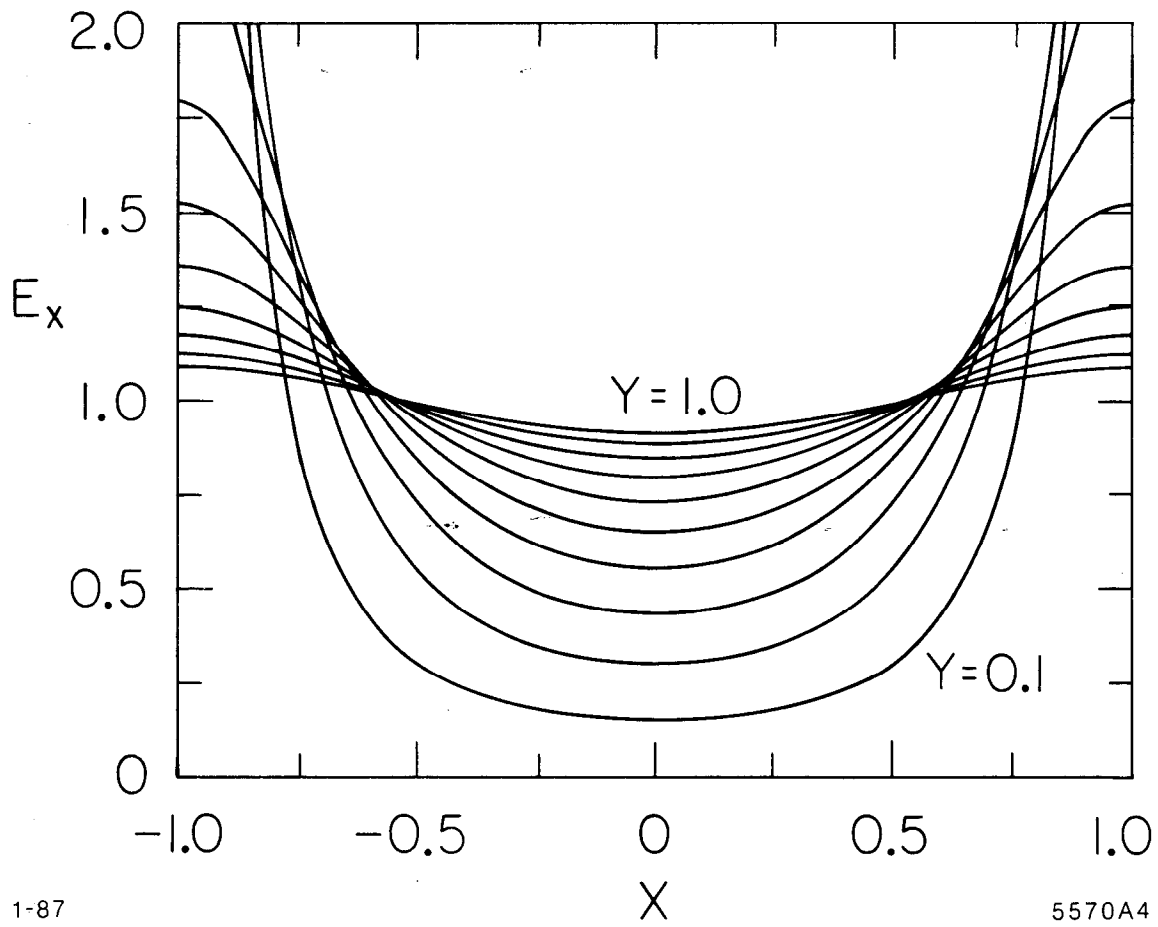
$N = 1$



$N = 3$

5570A3

Fig. 3



1-87

5570A4

Fig. 4

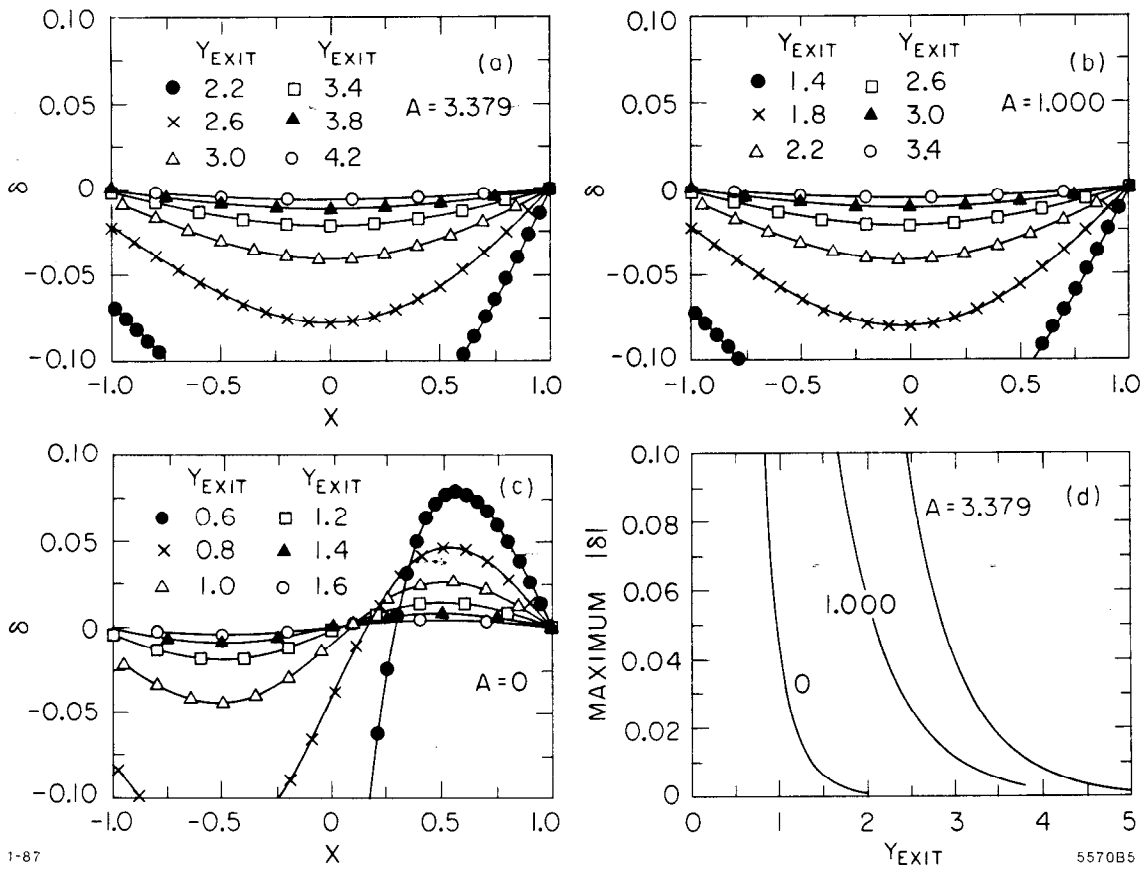
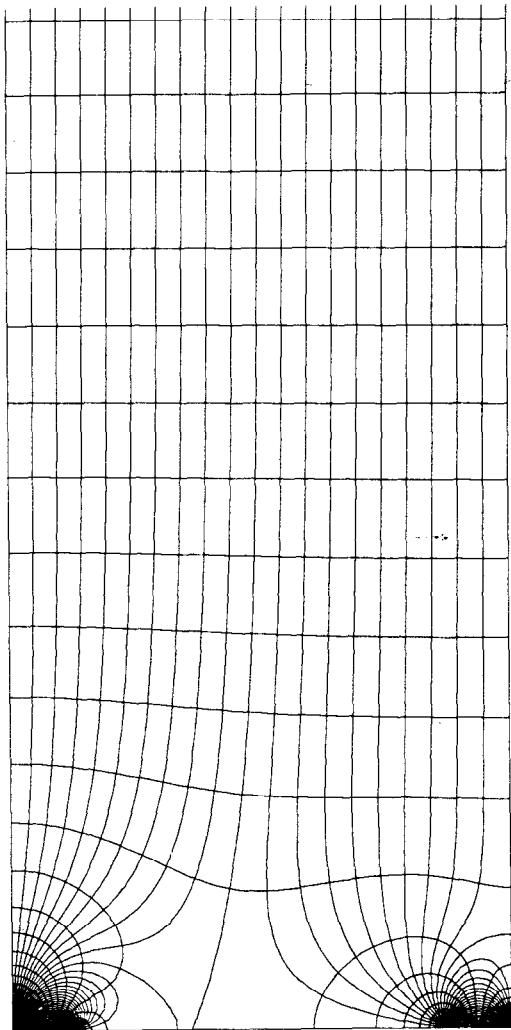
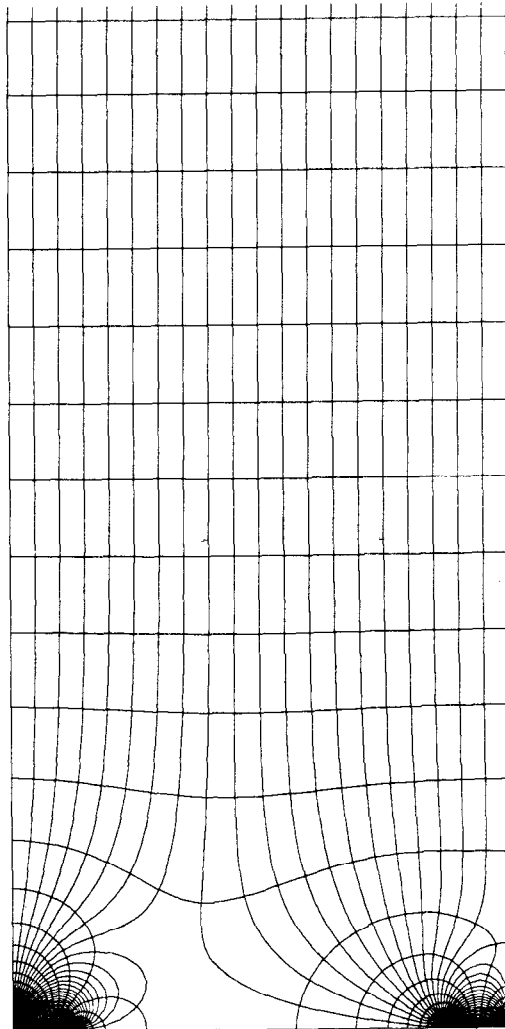


Fig. 5



$A=3.38, B=0, P=0.75$

1-87



$A=3.38, B=-0.28, P=0.75$

5570A6

Fig. 6

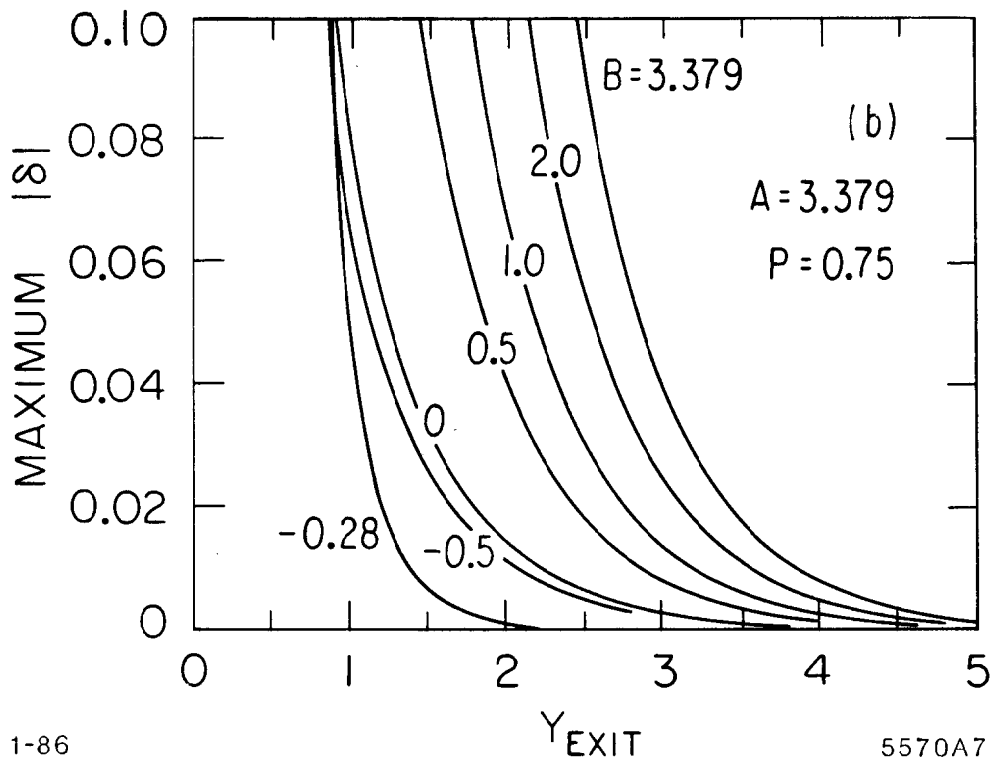
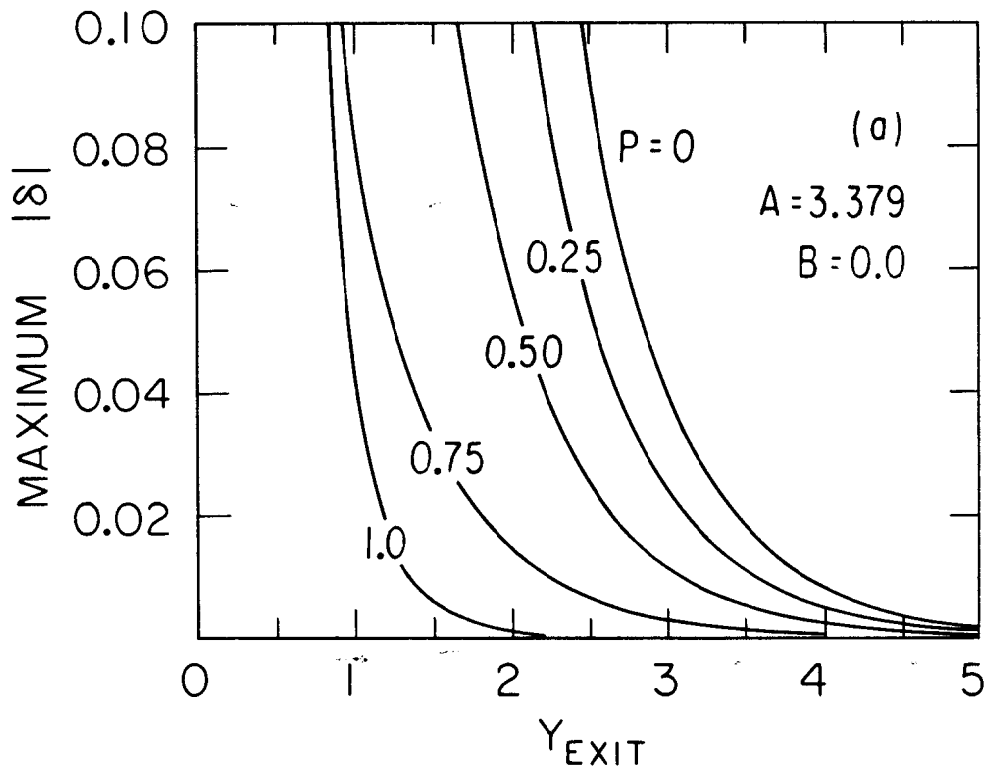
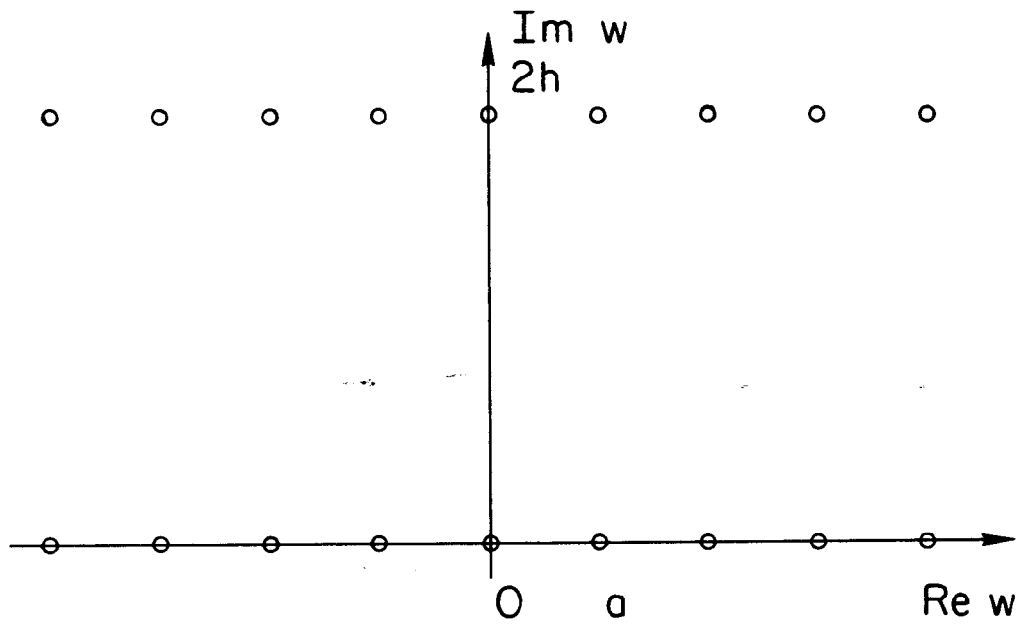


Fig. 7



1-87

5570A8

Fig. 8